Structural Properties of Hydrolyzed High-Amylose Rice Starch by α-Amylase from *Bacillus licheniformis*

Fengling Qin,[†] Jianmin Man,[†] Bin Xu,[‡] Maozhi Hu,[‡] Minghong Gu,[†] Qiaoquan Liu,[*,†] and Cunxu Wei[*,†]

[†]Key Laboratories of Crop Genetics and Physiology of the Jiangsu Province and Plant Functional Genomics of the Ministry of Education and [‡]Testing Center, Yangzhou University, Yangzhou 225009, People's Republic of China

ABSTRACT: High-amylose cereal starch has a great benefit on human health through its resistant starch (RS) content. Enzyme hydrolysis of native starch is very helpful in understanding the structure of starch granules and utilizing them. In this paper, native starch granules were isolated from a transgenic rice line (TRS) enriched with amylose and RS and hydrolyzed by α-amylase. Structural properties of hydrolyzed TRS starches were studied by X-ray powder diffraction, Fourier transform infrared, and differential scanning calorimetry. The A-type polymorph of TRS C-type starch was hydrolyzed faster than the B-type polymorph, but the crystallinity did not significantly change during enzyme hydrolysis. The degree of order in the external region of starch granule increased with increasing enzyme hydrolysis time. The amylose content decreased at first and then went back up during enzyme hydrolysis. The hydrolyzed starches exhibited increased onset and peak gelatinization temperatures and decreased gelatinization enthalpy on hydrolysis. These results suggested that the B-type polymorph and high amylose that formed the double helices and amylose−lipid complex increased the resistance to BAA hydrolysis. Furthermore, the spectrum results of RS from TRS native starch digested by pancreatic α-amylase and amyloglucosidase also supported the above conclusion.

KEYWORDS: Rice, high-amylose starch granule, α-amylase, structural property, enzyme hydrolysis

■ INTRODUCTION

Cereal storage starch is a major source of nourishment for humans. It is a mixture of two polysaccharides, linear amylose and highly branched amylopectin, and contains small amounts of noncarbohydrate constituents such as lipid, phosphate, and protein. Native starch is stored as a discrete semicrystalline granule in plants.[1] Depending on the botanical origin, native starches display different X-ray powder diffraction (XRD) patterns: an A type for normal cereal starches and a B type for tuber and high-amylose cereal starches. As a result of the presence of both A- and B-type crystallites in starch granules, legume starches are considered to present a C-type pattern.[2]

From a biological point of view, starch is basically a means of energy storage, so that its availability when degraded by amylases is an important tissue. For nutritional purposes, starch is classified into three types: rapidly digestible starch, slowly digestible starch, and resistant starch (RS).[3] RS is a portion of starch that cannot be hydrolyzed in the upper gastrointestinal tract and functions as a substrate for bacterial fermentation in the large intestine.[3] RS has been reported to provide many health benefits for humans; for example, RS-enriched food can lower the glycemic and insulin responses and reduce the risk for developing type II diabetes, obesity, and cardiovascular disease.[4] In general, the RS content of granular starch is positively correlated with the level of amylose.[5] So, many high-amylose crop varieties have been developed via mutation or transgenic breeding approaches.[6−8] Some of them have been proven to contain a high level of RS and show potential health benefits. For example, high amylose barley and wheat grains have a significant potential to improve health by the reduction of plasma cholesterol and production of increased large-bowel, short-chain fatty acids.[7,8]

Starch branching enzymes (SBEs) are responsible for the production of the α-1,6-glucosidic linkages in amylopectin, and at least three isoforms of SBEs (SBEI, SBEIIa, and SBEIIb) have been identified in rice endosperm. A high-amylose transgenic rice line (TRS) has been developed by antisense RNA inhibition of SBEI and SBEIIb.[9,10] TRS grains are rich in RS and have shown significant potential to improve the health of the large bowel in rats.[9] Our results from microstructure and ultrastructure studies reveal that TRS starch is a semicompound starch granule, which consists of many subgranules surrounded by a continuous band, whereas its wild-type rice Teqing starch is a compound starch granule.[10] Interestingly, TRS starch is identified as a C-type crystalline, which has a high resistance to acid hydrolysis, digestion, and heating.[11−13]

Most uses of starch in food and nonfood (pharmaceutics, papers, adhesives, packaging, biofuels, etc.) applications require the disruption of the starch granules through acid, alkaline, enzyme, or hydrothermal treatments (gelatinization/melting).[14,15] Enzyme hydrolysis of native starch is involved in many biological and industrial processes, such as starch metabolism in plants, digestion by mammals, malting, fermentation, glucose syrup, or bioethanol production. Starch is specifically hydrolyzed by amylolytic enzymes, which can cut either one or both types of glycosidic bonds. Among these enzymes, α-amylase is the main enzyme involved in the hydrolysis of α-1,4-bonds.[15,16] Native starch is digested (i.e., hydrolyzed) slowly as compared with processed (gelatinized) starch whose crystalline has been largely

destroyed and where the accessibility of substrate to enzymes is greater and not restricted by α-glucan associations such as double helices (especially in crystallites) or amylose−lipid complexes (in cereal starches).[17] Therefore, investigating the enzyme hydrolysis of native starch is essential to ensure fitness for purpose for a diverse range of end uses. Many researchers have reported the structure and physical properties of A-type and B-type starches as affected by enzyme hydrolysis, with the B-type crystalline being more resistant to enzyme hydrolysis than the A-type crystalline.[18] However, there is little information on the enzyme hydrolysis of the C-type starch.

In this paper, native TRS starch was hydrolyzed by α-amylase from *Bacillus licheniformis* (BAA) or by pancreatic α-amylase (PAA) and amyloglucosidase (AMG). The objective of this study is to characterize the hydrolyzed starch residues.

■ MATERIALS AND METHODS

Plant Material. A TRS with high amylose and RS contents was used in this study. TRS was generated from an *indica* rice cultivar Teqing after transgenic inhibition of two SBEs (SBEI and SBEIIb) through an antisense RNA technique and was homozygous for the transgene. The expressions of SBEI and SBEIIb were completely inhibited in TRS grains.[9] The apparent amylose content was dramatically increased from 22.7 to 49.2% in milled rice flour[10] and from 30.0 to 58.3% in isolated native starch,[11] and the RS content was increased from 1.9 to 14.9% in milled rice flour.[10] TRS was cultivated in the transgenic close experiment field of Yangzhou University, Yangzhou, China, in 2010, and mature grains were used to isolate starch granules.

Isolation of Native Starch Granules. Native starch granules were isolated from mature TRS grains as previously described.[11]

Hydrolysis of Starch Granules by α-Amylase. The hydrolyzed starch granules were prepared according to the method described by Wei et al.[11] with a slight modification. Isolated native starch (500 mg) was suspended in 50 mL of 0.1 M phosphate sodium buffer (pH 6.9) containing 0.006 M NaCl. BAA (Sigma-Aldrich) was added, with a final concentration of 0.01% (w/v). The amylolysis was carried out in a constant temperature shaking water bath at 37 °C with continuous shaking (100 rpm). After the desired time of hydrolysis, undissolved residues were quickly obtained by centrifugation (3000g, 10 min) at 4 °C, and the supernatant was used for measurement of the solubilized carbohydrates to quantify the degree of hydrolysis by the anthrone-H_2SO_4 method. The residues were subsequently washed three times with ddH_2O to remove residual enzyme and two times with acetone to dehydrate the residues and then dried at 40 °C for 2 days. Control starch without enzyme but incubated in the same enzymatic solution with the above experimental conditions for 96 h were run concurrently. The dried starches were ground into powders in a mortar with pestle and passed through a 100 mesh sieve for further property analysis.

RS Preparation. The preparation of RS was carried out with the Megazyme Resistant Starch Assay Kit with a slight modification. One gram of native starch sample was digested with 40 mL of PAA (10 mg/mL) containing AMG (3 U/mL) at 37 °C with continuous shaking (100 rpm) in a constant-temperature shaking water bath for 16 h. Undigested RS was obtained by centrifugation (3000g, 10 min), subsequently washed three times with ddH_2O and two times with acetone, and then dried at 40 °C for 2 days. Control starch without enzyme but subjected to the above experimental conditions was run concurrently. The dried starches were ground into powders in a mortar with pestle and passed through a 100 mesh sieve for XRD and attenuated total reflectance-Fourier transform infrared (ATR-FTIR) analyses.

XRD Analysis. XRD analysis of starches was carried out on an XRD (D8, Bruker, Germany), and the relative crystallinity (%) of the starches
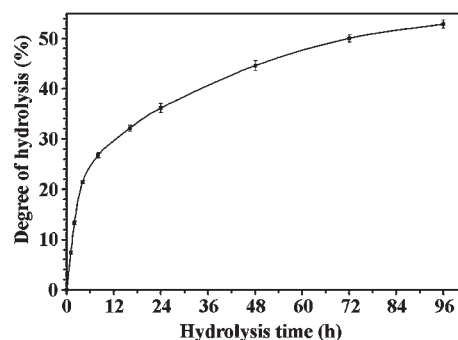

Figure 1. Hydrolysis of TRS starch by BAA.

was measured following the method described by Wei et al.[12] Before measurements, all of the specimens were stored in a desiccator where a saturated solution of NaCl maintained a constant humidity atmosphere (relative humidity = 75%) for 1 week.

ATR-FTIR Analysis. ATR-FTIR analysis of starches was carried out on a Varian 7000 FTIR spectrometer with a DTGS detector equipped with a ATR single reflectance cell containing a germanium crystal (45° incidence-angle) (PIKE Technologies, United States) as previously described.[11] Spectra were corrected by a baseline in the region from 1200 to 800 cm^{-1} before deconvolution was applied using Resolutions Pro. The assumed line shape was Lorentzian with a half-width of 19 cm^{-1} and a resolution enhancement factor of 1.9. Intensity measurements at 1047, 1022, and 995 cm^{-1} were performed on the deconcoluted spectra by recording the height of the absorbance bands from the baseline using Adobe Photoshop 7.0 image software.

Differential Scanning Calorimetry (DSC) Analysis. A DSC (200-F3, NETZSCH, Germany) was used to examine the thermal properties of starches as described previously.[13]

Amylose Content Measurement. The amylose content was determined using the Megazyme Amylose/Amylopectin Assay Kit, which is based on the precipitation of amylopectin using concanavalin A. The analysis was performed according to the instructions supplied with the kit.

Statistical Analysis. All analyses were replicated at least twice, and mean values and standard deviation values are reported. Analysis of variance (ANOVA) by Tukey's test ($p < 0.05$) was evaluated using the SPSS 16.0 Statistical Software Program.

■ RESULTS AND DISCUSSION

Hydrolysis Kinetics of TRS Starch by BAA. The time course of BAA hydrolysis of TRS starch is presented in Figure 1. The hydrolysis was biphasic, a relatively rapid rate at the initial stage (0−4 h), followed by a progressively decreased rate thereafter. A biphasic α-amylase hydrolysis trend has also been observed in legume starches with an initial rapid hydrolysis of the amorphous region followed by a decreased hydrolysis.[19] TRS starch has a high resistance to BAA hydrolysis.[11] After 96 h of hydrolysis, the extent of hydrolysis was only about 53% for TRS starch (Figure 1), which was significantly lower than that of its wild-type rice starch.[11]

Amylase hydrolysis involves an enzyme in solution acting on a solid starch substrate. Thus, the surface area accessible to enzyme and the efficiency of adsorption of enzyme onto this surface are critical kinetic parameters.[20] Starch granules from the regular rice are organized as compound starches and dissociated to individual starch subgranules during starch isolation. However, starch granules from TRS are organized as semicompound starches with a thick continuous band encircling the entire circumference

of the granules. The sizes of TRS semicompound starch granules are larger than those of regular rice starch subgranules.[10] Larger TRS starch granules have a lower granule surface area to volume, so TRS starches have a lower rate of enzyme hydrolysis than regular rice starches. It is also reported that the amount of native starch hydrolysis by amylase is inversely related to the amylose content.[21] The higher amylose content of TRS starch, which is nearly twice as much as that of its wild-type rice starch,[11] resists enzyme hydrolysis. Otherwise, the A-, B-, and C-type starches show different susceptibilities to α-amylase hydrolysis. Generally, the B- or C-type starch shows more resistance to enzyme hydrolysis than the A-type starch.[22] The C-type starch from TRS also has a higher resistance to α-amylase hydrolysis than the A-type starch from regular rice. Thus, as compared with regular rice starch, larger granule size, higher amylose content, and C-type crystalline in TRS starch lead to higher resistance to BAA.

The fluorophore molecular probe APTS specifically reacts with the reducing end of starch molecules and enables the distinction of the distribution of amylose and amylopectin in starch granule by confocal laser scanning microscopy.[23] Analysis of APTS-labeled starch granules demonstrates that regular rice starch granules have a high concentration of amylose in the concentric hilum, whereas TRS starch granules show a relatively even distribution of amylose with intense amylose in both hilum and band encircling the entire circumference of the granules.[10] The content of amylose—lipid complex that has a high resistance to amylase hydrolysis is higher in TRS starch than that in regular rice starch.[11] Although TRS starch has a high amylose content, the amylose distribution and amylose—lipid complex resulted in a higher resistance to BAA hydrolysis.

XRD Spectra of Hydrolyzed Starches by BAA. To exclude the effect of enzyme solution (0.1 M phosphate sodium buffer, pH 6.9) on the structural properties, we used control starch instead of native starch. The XRD pattern and relative crystallinity of control and hydrolyzed starches are shown in Figure 2. The XRD spectrum of native starch (not shown) was similar to that of the control starch. Starches can be classified to A-, B-, and C-type crystalline by XRD pattern. The A-type crystal starches have strong diffraction peaks at about 15° and 23° 2θ and an unresolved doublet at around 17° and 18° 2θ. The B-type crystal starches give the strongest diffraction peak at around 17° 2θ, a few small peaks at around 15°, 20°, 22°, and 24° 2θ, and a characteristic peak at about 5.6° 2θ. The C-type crystal starch is a mixture of both A- and B-type crystalline and can be further classified to C_A type (closer to A type), C type, and C_B type (closer to B type) according to the proportion of A-type and B-type polymorphs. The typical C-type crystal starches show strong diffraction peaks at about 17° and 23° 2θ and a few small peaks at around 5.6° and 15° 2θ. The XRD patterns of C_A- and C_B-type crystal starches show some slight differences from that of typical C type. C_A-type crystal starches show a shoulder peak at about 18° 2θ and strong peaks at about 15° and 23° 2θ, which are indicative of the A-type pattern. C_B-type crystal starches show two shoulder peaks at about 22° and 24° 2θ and a weak peak at about 15° 2θ, which are indicative of the B-type pattern. The peak at 20° 2θ was the amylose—lipid complex diffraction peak. The peak at 15° 2θ is strongest in A-type crystalline and weakest in B-type crystalline.[2]

TRS control starch showed a C-type XRD pattern characterized by strong diffraction peaks at about 15°, 17°, and 23° 2θ, weak diffraction peaks at around 5.6° and 20° 2θ, and a shoulder peak at 18° 2θ (Figure 2). The peak at around 5.6° 2θ is
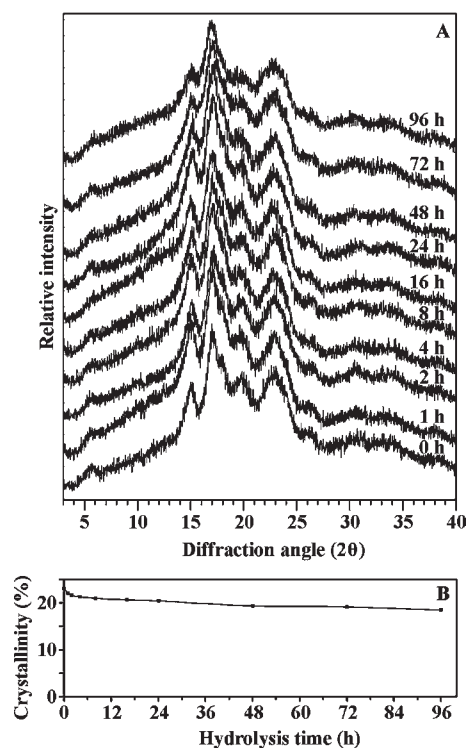
Figure 2. XRD spectra and the degree of crystallinity of hydrolyzed TRS starch by BAA for different times. (A) XRD spectra and (B) degree of crystallinity.

characteristic of the B-type pattern, while the peak at 23° 2θ and the shoulder peak at 18° 2θ are indicative of the A-type pattern.[2,11] Although TRS control and hydrolyzed starches all remained in a similar pattern, it was noteworthy that the intensity of the shoulder peak at 18° 2θ was found to decrease, the peak at 23° 2θ became shorter, and the peak at 15° 2θ became weaker with increasing BAA hydrolysis time (Figure 2A). The diffraction intensity variations of peaks at 15°, 18°, and 23° 2θ indicated that the ratio of B/A polymorph progressively increased in hydrolyzed TRS starch residues. That was to say, the A-type polymorph was degraded more rapidly than the B-type polymorph during BAA hydrolysis.

Native waxy rice starch exhibits a typical A-type XRD pattern. Hydrolysis with the α-amylase does not change the XRD pattern, but more extensive hydrolysis substantially decreases the diffraction intensity.[24] The crystalline of B-type starch does not markedly change after enzyme hydrolysis.[25] TRS starch is C-type crystalline, a mixture of A-type and B-type polymorphs.[11] In this study, the A-type polymorph was hydrolyzed faster than the B-type polymorph, which was in agreement with Jane et al.'s[18] report but different from Jiang et al.'s[25] results. Jiang et al.'s[25] study shows that *Dioscorea opposita* Thunb. starch is C-type crystalline, and the B-type polymorph is preferentially degraded or degraded faster than the A-type polymorph. In TRS starch, the A-type polymorph is located at the central part of subgranule and is surrounded by the B-type polymorph at the peripheral region of subgranules and the surrounding band of starch granule.[12] However, in *D. opposita* starch, the B-type polymorph is located at the central part of granule and is surrounded by an A-type polymorph at the granule periphery.[25] Electron microscopy has revealed that α-amylase pits the granule surface first and then
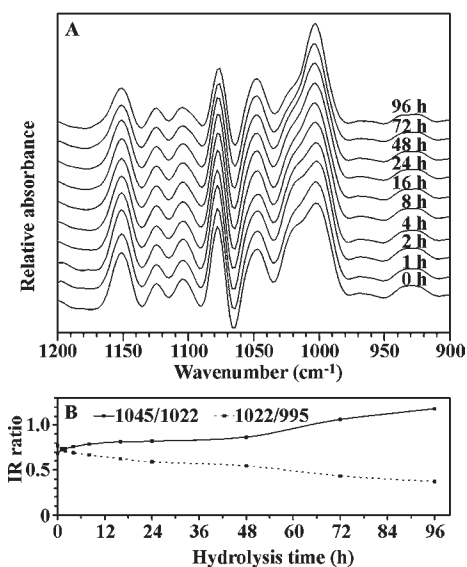
Figure 3. ATR-FTIR spectra of hydrolyzed TRS starch by BAA for different times. (A) Deconvoluted spectra and (B) the IR ratio of absorbances 1045/1022 and 1022/995 cm^{-1}.

Figure 4. XRD spectra of digested TRS starch by PAA and AMG for 16 h. (A) Control starch and (B) RS.

penetrates through pinholes/internal channels and hydrolyzes the granule from inside-out.[26] So, it is easy to understand the differences of polymorph degradation in C-type *D. opposita* and TRS starches in view of the polymorph location in starch granule.

There was no significant change in the relative crystallinity during BAA hydrolysis (Figure 2B), which indicated that the amorphous and crystalline components of starch granule were hydrolyzed at a similar rate. Several researchers have shown that both amorphous and semicrystalline regions of starch granules are hydrolyzed simultaneously by α-amylases, which is based on the observation that α-amylolysis does not produce a marked increase in the crystallinity.[19,27]

ATR-FTIR Spectra of Hydrolyzed Starches by BAA. The development of sampling devices like ATR-FTIR combined with procedures for spectrum deconvolution provides opportunities for the study of starch structure.[28] According to the theory of ATR, the penetration depth is related to the wavelength. Polysaccharides, like starch, absorb in the region 1200–800 cm^{-1}, that is, at a wavelength between ~8 and 12 μm. In this region, the average penetration depth is ~2 μm. Therefore, ATR-FTIR is used to study the external region of starch granule. Although FTIR is not able to differentiate between A- and B-type crystalline, the variation between starch varieties is interpreted in terms of the level of ordered structure present on the edge of starch granules.[28]

The deconvoluted ATR-FTIR spectra in the region 1200–900 cm^{-1} of control and hydrolyzed starches are presented in Figure 3A. The XRD spectrum of native starch (not shown) was similar to that of control starch. The bands at 1045 and 1022 cm^{-1} are linked with the ordered and amorphous structures of starch granule, respectively. The ratio of absorbance 1045/1022 cm^{-1} is used to quantify the degree of order in starch samples.[22] Intensity ratios of 1045/1022 and 1022/995 cm^{-1} are useful as a convenient index of FTIR data in comparison with other measures of starch conformation.[29] The relative intensities of FTIR bands of TRS starches at 1045, 1022, and 995 cm^{-1} were measured, and the ratios of 1045/1022 and 1022/995 cm^{-1} were calculated as shown in Figure 3B. On the basis of both the spectra
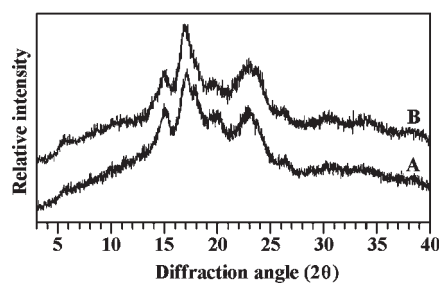
and the calculated data, the degree of order in the external region of starch granule increased with enzyme hydrolysis. This could partly explain the biphasic BAA hydrolysis trend with the ordered structure being more resistant to enzyme hydrolysis than the amorphous structure. With increasing hydrolysis time, the ordered structure in the external region of starch granule increased; therefore, the hydrolysis rate decreased thereafter.

Molecular order in a starch granule is composed of two types of helices from amylopectin side chains. Helices that are packed in regular arrays or in the long-range order form crystalline. Helices that are not packed in regular form or packed in the short-range order form the so-called double helical order.[30] XRD detects the long-range order, and FTIR measures the short-range order. ATR-FTIR can provide information on the ratio of double helical ordered to amorphous fraction at the external region of starch granule.[28] It is therefore not surprising that estimates of order proportion by XRD are considerably different from those by ATR-FTIR. In this study, the relative crystallinity slightly decreased by XRD analysis (Figure 2), which indicated that there is not preferential hydrolysis of either a long-range ordered or an amorphous fraction in TRS starch by BAA. The ratio of absorbances 1045/1022 cm^{-1} significantly increased by ATR-FTIR analysis (Figure 3), which indicated that the amorphous structure is degraded faster by BAA than the double helical ordered structure at the external region of the TRS starch granule.

XRD and FTIR Spectra of RS from TRS Starch Digested by PAA and AMG. To further confirm the XRD and ATR-FTIR results of hydrolyzed starches by BAA, we prepared RS from native TRS starch according to the Megazyme Resistant Starch Assay Kit. Native TRS starch was digested by PAA and AMG at 37° for 16 h, and RS was obtained. The XRD spectra of control and RSs are shown in Figure 4. The XRD spectrum of native starch (not shown) was similar to that of control starch. The results were similar to those of hydrolyzed starches by BAA. As compared with control starch, the XRD pattern of RS indicated that the shoulder peak at 18° 2θ decreased, the peak at 23° 2θ became broad, and the intensity of peak at 5.6° 2θ increased. This result also showed that an A-type polymorph was degraded more rapidly than a B-type polymorph during TRS starch digestion by PAA and AMG. The relative crystallinity of RS slightly decreased (Table 1), which is similar to hydrolyzed starch by BAA (Figure 2).

The ATR-FTIR spectra of control and RSs are presented in Figure 5. The spectrum of native starch (not shown) was similar to that of control starch. The results were also similar to those of hydrolyzed starches by BAA. On the basis of both the spectra and the calculated data of RS (Figure 5 and Table 1), the degree of order in the external region of RS granule increased. This could explain the high resistance of RS to enzyme digestion.

Table 1. Crystallinity and IR Ratio of RS Prepared from TRS Starch Digested by PAA and AMG for 16 h[a]

starch	relative crystallinity (%)	IR ratio (cm^{-1})	
		1045/1022	1022/995
control starch[b]	22.58 ± 0.71 a	0.67 ± 0.05 a	0.74 ± 0.06 a
RS	20.81 ± 0.65 a	1.08 ± 0.08 b	0.47 ± 0.05 b

[a] Data (means ± SDs) in the same column with different letters are significantly different ($p < 0.05$). [b] Treated without enzyme but subjected to the same experimental conditions.
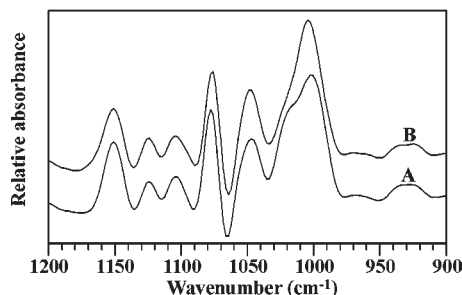
Figure 5. ATR-FTIR deconvoluted spectra of digested TRS starch by PAA and AMG for 16 h. (A) Control starch and (B) RS.

The hydrolysis rate of TRS starch by PAA and AMG was significantly higher than by BAA. The degree of hydrolysis by PAA and AMG for 16 h reached 85.1%.[10] However, the extent of hydrolysis by BAA for 16 h was only about 32.1% (Figure 1). This result is in agreement with Fujii and Kawamura's[31] study. There is a synergistic action of α-amylase and glucoamylase on hydrolysis of starch. At the early stage of the reaction, α-amylase acts as a contributor of newly formed nonreducing ends of starch molecules to glucoamylase by splitting the original starch molecules.[31] Although 16 h RS and BAA hydrolyzed starch residues showed similar XRD patterns, it was noteworthy that the intensity of peak at 5.6° 2θ, which is characteristic of the B-type XRD pattern, was significantly higher in 16 h RS than that in 16 h BAA hydrolyzed starch residues (Figures 2 and 4), which indicated that the ratio of B/A polymorph was higher in 16 h RS than in 16 h BAA hydrolyzed starch residues. That is to say, as compared with the B-type polymorph, the A-type polymorph was degraded faster by PAA and AMG than by BAA. Sixteen hour RS and BAA hydrolyzed starch residues had a similar crystallinity (Figure 2 and Table 1), which indicated that the amorphous and crystalline starch was degraded at a similar rate by PAA and AMG and by BAA. ATR-FTIR results showed that the absorbance intensity at 1022 cm^{-1} was significantly lower, and the ratio of absorbances 1045/1022 cm^{-1} was significantly higher in 16 h RS than in 16 h BAA hydrolyzed starch residues, which indicated that the amorphous structure was degraded faster by PAA and AMG than by BAA, which resulted in the higher ratio of double helical ordered to amorphous structure in 16 h RS at the external region of TRS starch granule.

Amylose Content of Hydrolyzed Starches by BAA. The amylose content of hydrolyzed starches by BAA was determined using the Megazyme Amylose/Amylopectin Assay Kit, and the results are presented in Table 2. The amylose content decreased at initial hydrolysis (1−4 h) and then gradually increased with increasing hydrolysis time. In the starch granule, some amylose

Table 2. Amylose Contents of Hydrolyzed TRS Starch by BAA for Different Times

hydrolysis time (h)	amylose content (%)
0[a]	51.6 ± 1.6 c
1	43.5 ± 1.2 b
2	40.3 ± 0.9 ab
4	39.3 ± 0.9 a
8	40.6 ± 0.6 ab
16	40.5 ± 0.5 ab
24	40.0 ± 1.4 ab
48	43.5 ± 0.5 b
72	48.3 ± 0.7 c
96	55.8 ± 1.5 d

[a] Control starch, which is treated without α-amylase but subjected to the same experimental conditions for 96 h in enzymatic solution, is equivalent to 0 h of BAA hydrolysis. Data (means ± SDs) in the same column with different letters are significantly different ($p < 0.05$).

forms the double helix, some amylose and lipid form the amylose−lipid complex, and the other amylose is located in the starch amorphous region. The double helices associate to form crystalline. The amount of double helices in starch granule exceeds the amount of crystalline. This is because not all double helices are involved in crystallites.[32] The crystalline and double helices themselves resist the enzyme hydrolysis.[22] The amylose−lipid complex has a high resistance to amylase hydrolysis;[33] however, the starch amorphous region is less resistant to digestion. Thus, starch enzyme hydrolysis has an initial rapid hydrolysis of the amorphous regions followed by a slow hydrolysis of ordered structure. The decrease in amylose content at first is due to the fact that the hydrolysis of amorphous starch was faster than that of ordered structure. The increase in amylose content at later hydrolysis is due to the fact that the hydrolysis of ordered structure from amylopectin side chains was faster than that of double helical amylose and amylose−lipid complex.

The amylose forms the double helices and amylose−lipid complex, which have high resistance to amylase hydrolysis. This probably (at least in part) explains why high amylose starches resist amylase digestion, even though they are less crystalline.[21] In this paper, the slight decrease of crystallinity in hydrolyzed TRS starch residues (Figure 2) indicated that the crystalline was degraded. The significant increase in the ratio of absorbance 1045/1022 cm^{-1} (Figure 3) indicated that the double helices have high resistance to hydrolysis. Therefore, we speculate that the higher amylose content resulting from the double helices and amylose−lipid complex in hydrolyzed TRS starch residues increased the resistance to BAA hydrolysis.

Thermal Properties of Hydrolyzed Starches by BAA. The thermal properties of starch granules are usually measured by DSC. The thermal properties of control and BAA hydrolyzed starches are summarized in Table 3. The onset and peak gelatinization temperatures increased, and the range of gelatinization temperature and the endothermic values decreased with increasing enzyme hydrolysis time (Table 3). The normal corn and potato starches also exhibit increased peak gelatinization temperature and decreased endothermic values on hydrolysis by α-amylase.[34] The peak gelatinization temperature provides a measure of ordered structure quality. Its increase indicates hydrolysis of the amorphous structure by enzymes because the amorphous regions facilitate the melting of ordered structure.[35] TRS starch

Table 3. Thermal Properties of Hydrolyzed TRS Starch by BAA for Different Times

hydrolysis time (h)	°C[a]				ΔH (J/g)[a]
	T_o	T_p	T_c	ΔT	
0[b]	70.4 ± 0.3 a	79.6 ± 0.2 a	89.7 ± 0.2 bc	19.3 ± 0.1 b	9.1 ± 0.5 f
1	72.9 ± 0.2 b	80.3 ± 0.3 ab	88.8 ± 0.5 abc	15.9 ± 0.7 a	6.1 ± 0.3 bc
2	72.6 ± 0.1 b	80.3 ± 0.2 ab	88.8 ± 0.3 abc	16.2 ± 0.4 a	7.0 ± 0.2 ce
4	72.7 ± 0.3 b	80.0 ± 0.2 ab	88.5 ± 0.2 a	15.8 ± 0.6 a	8.7 ± 0.2 f
8	72.5 ± 0.1 b	80.7 ± 0.3 bd	88.4 ± 0.3 a	15.9 ± 0.4 a	7.3 ± 0.3 de
16	72.8 ± 0.2 b	80.6 ± 0.3 abc	88.4 ± 0.2 a	15.6 ± 0.4 a	6.5 ± 0.2 bcd
24	72.7 ± 0.2 b	81.4 ± 0.4 cde	88.7 ± 0.3 ab	16.0 ± 0.1 a	5.9 ± 0.2 b
48	72.8 ± 0.2 b	80.5 ± 0.2 abc	89.0 ± 0.4 ac	16.2 ± 0.6 a	6.7 ± 0.3 bcd
72	74.3 ± 0.3 c	81.9 ± 0.3 e	89.9 ± 0.5 c	15.6 ± 0.8 a	5.6 ± 0.2 b
96	73.9 ± 0.4 c	82.3 ± 0.4 e	88.5 ± 0.3 a	14.6 ± 0.7 a	4.4 ± 0.3 a

[a] T_o, onset temperature; T_p, peak temperature; T_c, conclusion temperature; ΔT, gelatinization range ($T_c - T_o$); ΔH, enthalpy of gelatinization. [b] Control starch, which is treated without α-amylase but is subjected to the same experimental conditions for 96 h in enzymatic solution, is equivalent to 0 h of BAA hydrolysis. Data (means ± SDs) in the same column with different letters are significantly different ($p < 0.05$).

showed an increase in peak gelatinization temperature on hydrolysis. These results suggested that hydrolyzed starch residues had a more ordered and stable structure. Therefore, the melting of these ordered structure occurred at a higher temperature. The range of gelatinization temperature has been reported to be dependent on the degree of heterogeneity of crystallites within the starch granules, and the endothermic values are associated with the disruption of double helices rather than with the crystalline order of the granules.[35] The reduction in endothermic values (Table 3) supported the hydrolysis of the crystalline and helical structure.[36] The increase in peak gelatinization temperature and the reduction in endothermic values suggested that both amorphous and crystalline structure of TRS starch were hydrolyzed by BAA, which was in agreement with results of Colonna et al.,[37] and both amylose and amylopectin are hydrolyzed by α-amylase.

In conclusion, the structural properties of hydrolyzed TRS starch by α-amylase were investigated by using XRD, ATR-FTIR, and DSC techniques. These results indicated that the A-type polymorph of TRS C-type starch was more easily degraded than the B type. The amylose that forms the double helices and amylose—lipid complex increased the resistance to enzyme hydrolysis. These data could add to our understanding of the effect of enzyme hydrolysis on the high-amylose rice starch and would be very helpful for application of high-amylose RS rice in food and nonfood industries.

■ AUTHOR INFORMATION

Corresponding Author
*Tel: +86 514 87996648. E-mail: qqliu@yzu.edu.cn (Q.L.). Tel: +86 514 87997217. E-mail: cxwei@yzu.edu.cn (C.W.).

■ ABBREVIATIONS USED

AMG, amyloglucosidase; ATR-FTIR, attenuated total reflectance-Fourier transform infrared; BAA, α-amylase from *Bacillus licheniformis*; DSC, differential scanning calorimetry; PAA, pancreatic α-amylase; RS, resistant starch; SBE, starch branching enzyme; TRS, transgenic rice line; XRD, X-ray powder diffraction

■ REFERENCES

(1) Gallant, D. J.; Bouchet, B.; Baldwin, P. M. Microscopy of starch: Evidence of a new level of granule organization. *Carbohydr. Polym.* **1997**, *32*, 177–191.

(2) Cheetham, N. W. H.; Tao, L. Variation in crystalline type with amylose content in maize starch granules: An X-ray powder diffraction study. *Carbohydr. Polym.* **1998**, *36*, 277–284.

(3) Englyst, H. N.; Kingman, S. M.; Cummings, J. H. Classification and measurement of nutritionally important starch fractions. *Eur. J. Clin. Nutr.* **1992**, *46*, S33–S50.

(4) Nugent, A. P. Health properties of resistant starch. *Nutr. Bull.* **2005**, *30*, 27–54.

(5) Sang, Y. J.; Bean, S.; Seib, P. A.; Pedersen, J.; Shi, Y. C. Structure and functional properties of sorghum starches differing in amylose content. *J. Agric. Food Chem.* **2008**, *56*, 6680–6685.

(6) Schwall, G. P.; Safford, R.; Westcott, R. J.; Jeffcoat, R.; Tayal, A.; Shi, Y. C.; Gidley, M. J.; Jobling, S. A. Production of very-high-amylose potato starch by inhibition of SBE A and B. *Nat. Biotechnol.* **2000**, *18*, 551–554.

(7) Bird, A. R.; Jackson, M.; King, R. A.; Davies, D. A.; Usher, S.; Topping, D. L. A novel high-amylose barley cultivar (*Hordeum vulgare* var. *Himalaya 292*) lowers plasma cholesterol and alters indices of large-bowel fermentation in pigs. *Br. J. Nutr.* **2004**, *92*, 607–615.

(8) Regina, A.; Bird, A.; Topping, D.; Bowden, S.; Freeman, J.; Barsby, T.; Kosar-Hashemi, B.; Li, Z. Y.; Rahman, S.; Morell, M. High-amylose wheat generated by RNA interference improves indices of large-bowel health in rats. *Proc. Natl. Acad. Sci. U.S.A.* **2006**, *103*, 3546–3551.

(9) Zhu, L. J. Studies on starch structure and functional properties of high-amylose transgenic rice and different waxy rice varieties. Ph.D. dissertation, Yangzhou University, Yangzhou, China, 2009.

(10) Wei, C. X.; Qin, F. L.; Zhu, L. J.; Zhou, W. D.; Chen, Y. F.; Wang, Y. P.; Gu, M. H.; Liu, Q. Q. Microstructure and ultrastructure of high-amylose rice resistant starch granules modified by antisense RNA inhibition of starch branching enzyme. *J. Agric. Food Chem.* **2010**, *58*, 1224–1232.

(11) Wei, C. X.; Xu, B.; Qin, F. L.; Yu, H. G.; Chen, C.; Meng, X. L.; Zhu, L. J.; Wang, Y. P.; Gu, M. H.; Liu, Q. Q. C-type starch from high-amylose rice resistant starch granules modified by antisense RNA inhibition of starch branching enzyme. *J. Agric. Food Chem.* **2010**, *58*, 7383–7388.

(12) Wei, C. X.; Qin, F. L.; Zhou, W. D.; Yu, H. G.; Xu, B.; Chen, C.; Zhu, L. J.; Wang, Y. P.; Gu, M. H.; Liu, Q. Q. Granule structure and distribution of allomorphs in C-type high-amylose rice starch granule modified by antisense RNA inhibition of starch branching enzyme. *J. Agric. Food Chem.* **2010**, *58*, 11946–11954.

(13) Wei, C. X.; Qin, F. L.; Zhou, W. D.; Xu, B.; Chen, C.; Chen, Y. F.; Wang, Y. P.; Gu, M. H.; Liu, Q. Q. Comparison of the crystalline properties and structural changes of starches from high-amylose transgenic rice and its wild type during heating. *Food Chem.* **2011**, *128*, 645–652.

(14) Buléon, A.; Colonna, P. Physicochemical behaviour of starch in food applications. In *The Chemical Physics of Food*; Belton, P., Ed.; Blackwell Publishing: Oxford, United Kingdom, 2007; pp 20–59.

(15) Tawil, G.; Viksø-Nielsen, A.; Rolland-Sabaté, A.; Colonna, P.; Buléon, A. In depth study of a new highly efficient raw starch hydrolyzing α-amylase from *Rhizomucor sp. Biomacromolecules* **2011**, *12*, 34–42.

(16) Oates, C. G. Towards an understanding of starch granule structure and hydrolysis. *Trends Food Sci. Technol.* **1997**, *8*, 375–382.

(17) Blazek, J.; Gilbert, E. P. Effect of enzymatic hydrolysis on native starch granule structure. *Biomacromolecules* **2010**, *11*, 3275–3289.

(18) Jane, J. L.; Wong, K. S.; McPherson, A. E. Branch-structure difference in starches of A- and B-type X-ray patterns revealed by their Naegeli dextrins. *Carbohydr. Res.* **1997**, *300*, 219–227.

(19) Zhou, Y.; Hoover, R.; Liu, Q. Relationship between α-amylase degradation and the structure and physicochemical properties of legume starches. *Carbohydr. Polym.* **2004**, *57*, 299–317.

(20) Bertoft, E.; Manelius, R. A method for the study of the enzymatic hydrolysis of starch granules. *Carbohydr. Res.* **1992**, *227*, 269–283.

(21) Tester, R. F.; Qi, X.; Karkalas, J. Hydrolysis of native starches with amylases. *Anim. Feed Sci. Technol.* **2006**, *130*, 39–54.

(22) Tester, R. F.; Karkalas, J.; Qi, X. Starch structure and digestibility enzyme-substrate relationship. *World Poult. Sci. J.* **2004**, *60*, 186–195.

(23) Blennow, A.; Hansen, M.; Schulz, A.; Jørgensen, K.; Donald, A. M.; Sanderson, J. The molecular deposition of transgenically modified starch in the starch granule as imaged by functional microscopy. *J. Struct. Biol.* **2003**, *143*, 229–241.

(24) Kim, J. Y.; Park, D. J.; Lim, S. T. Fragmentation of waxy rice starch granules by enzymatic hydrolysis. *Cereal Chem.* **2008**, *85*, 182–187.

(25) Jiang, Q. Q.; Gao, W. Y.; Li, X.; Zhang, J. Z. Characteristics of native and enzymatically hydrolyzed *Zea mays* L., *Fritillaria ussuriensis* Maxim. and *Dioscorea opposita* Thunb. starches. *Food Hydrocolloids* **2011**, *25*, 521–528.

(26) Li, J. H.; Vasanthan, T.; Hoover, R.; Rossnagel, B. G. Starch from hull-less barley: V. In-vitro susceptibility of waxy, normal, and high-amylose starches towards hydrolysis by alpha-amylases and amyloglucosidase. *Food Chem.* **2004**, *84*, 621–632.

(27) Lauro, M.; Forssell, P. M.; Suortti, M. T.; Hulleman, S. H. D.; Poutanen, K. S. α-amylolysis of large barley starch granules. *Cereal Chem.* **1999**, *76*, 925–930.

(28) Sevenou, O.; Hill, S. E.; Farhat, I. A.; Mitchell, J. R. Organisation of the external region of the starch granule as determined by infrared spectroscopy. *Int. J. Biol. Macromol.* **2002**, *31*, 79–85.

(29) Htoon, A.; Shrestha, A. K.; Flanagan, B. M.; Lopez-Rubio, A.; Bird, A. R.; Gilbert, E. P.; Gidley, M. J. Effects of processing high amylose maize starches under controlled conditions on structural organisation and amylase digestibility. *Carbohydr. Polym.* **2009**, *75*, 236–245.

(30) Atichokudomchai, N.; Varavinit, S.; Chinachoti, P. A study of ordered structure in acid-modified tapioca starch by ^{13}C CP/MAS solid-state NMR. *Carbohydr. Polym.* **2004**, *58*, 383–389.

(31) Fujii, M.; Kawamura, Y. Synergistic action of α-amylase and glucoamylase on hydrolysis of starch. *Biotechnol. Bioeng.* **1985**, *27*, 260–265.

(32) Cooke, D.; Gidley, M. J. Loss of crystalline and molecular order during starch gelatinisation—origin of the enthalpic transition. *Carbohydr. Res.* **1992**, *227*, 103–112.

(33) Gérard, C.; Colonna, P.; Buléon, A.; Planchot, V. Amylolysis of maize mutant starches. *J. Sci. Food Agric.* **2001**, *81*, 1281–1287.

(34) O'Brien, S.; Wang, Y. J. Susceptibility of annealed starches to hydrolysis by α-amylase and glucoamylase. *Carbohydr. Polym.* **2008**, *72*, 597–607.

(35) Campanha, R. B.; Franco, C. M. L. Gelatinization properties of native starches and their Näegeli dextrins. *J. Therm. Anal. Calorim.* **2011**, DOI: 10.1007/s10973-011-1682-7.

(36) Sandhu, K. S.; Singh, N.; Lim, S. T. A comparison of native and acid thinned normal and waxy corn starches: physicochemical, thermal, morphological and pasting properties. *LWT—Food Sci. Technol.* **2007**, *40*, 1527–1536.

(37) Colonna, P.; Buléon, A.; Lemarié, F. Action of *Bacillus subtilis* α-amylase on native wheat starch. *Biotechnol. Bioeng.* **1988**, *31*, 895–904.